Deep-Sea Research I 102 (2015) 43–54

Contents lists available at ScienceDirect

Deep-Sea Research I

journal homepage: www.elsevier.com/locate/dsri

Water properties, heat and volume fluxes of Pacific water in Barrow Canyon during summer 2010

Motoyo Itoh [a,*], Robert S. Pickart [b], Takashi Kikuchi [a], Yasushi Fukamachi [c], Kay I. Ohshima [c], Daisuke Simizu [c,d], Kevin R. Arrigo [e], Svein Vagle [f], Jianfeng He [g], Carin Ashjian [b], Jeremy T. Mathis [h], Shigeto Nishino [a], Carolina Nobre [b]

[a] Japan Agency for Marine-Earth Science and Technology, Yokosuka, Kanagawa, Japan
[b] Woods Hole Oceanographic Institution, Woods Hole, MA 02543, USA
[c] Institute of Low Temperature Science, Hokkaido University, Sapporo, Japan
[d] National Institute of Polar Research, Tachikawa, Japan
[e] Department of Environmental Earth System Science, Stanford University, Stanford, CA 94305, USA
[f] Fisheries and Oceans Canada, Institute of Ocean Sciences, Sidney, British Columbia, Canada
[g] Polar Research Institute of China, Shanghai, China
[h] NOAA Pacific Marine Laboratory, Seattle, WA 98115, USA

ARTICLE INFO

Article history:
Received 16 July 2014
Received in revised form
9 April 2015
Accepted 11 April 2015
Available online 25 April 2015

Keywords:
Polar oceanography
Arctic Ocean
Chukchi Sea
Heat fluxes
Volume transports
Water properties

ABSTRACT

Over the past few decades, sea ice retreat during summer has been enhanced in the Pacific sector of the Arctic basin, likely due in part to increasing summertime heat flux of Pacific-origin water from the Bering Strait. Barrow Canyon, in the northeast Chukchi Sea, is a major conduit through which the Pacific-origin water enters the Arctic basin. This paper presents results from 6 repeat high-resolution shipboard hydrographic/velocity sections occupied across Barrow Canyon in summer 2010. The different Pacific water masses feeding the canyon – Alaskan coastal water (ACW), summer Bering Sea water (BSW), and Pacific winter water (PWW) – all displayed significant intra-seasonal variability. Net volume transports through the canyon were between 0.96 and 1.70 Sv poleward, consisting of 0.41–0.98 Sv of warm Pacific water (ACW and BSW) and 0.28–0.65 Sv of PWW. The poleward heat flux also varied strongly, ranging from 8.56 TW to 24.56 TW, mainly due to the change in temperature of the warm Pacific water. Using supplemental mooring data from the core of the warm water, along with wind data from the Pt. Barrow weather station, we derive and assess a proxy for estimating heat flux in the canyon for the summer time period, which is when most of the heat passes northward towards the basin. The average heat flux for 2010 was estimated to be 3.34 TW, which is as large as the previous record maximum in 2007. This amount of heat could melt 315,000 km^2 of 1-meter thick ice, which likely contributed to significant summer sea ice retreat in the Pacific sector of the Arctic Ocean.

1. Introduction

Pacific water enters the Arctic Ocean via Bering Strait and flows northward across the wide and shallow Chukchi Sea. The long-term mean annual transport measured at the strait is 0.8 Sv (1 Sv $=10^6\ m^3 s^{-1}$) (Roach et al., 1996; Woodgate et al., 2006), although recently this has increased to more than 1 Sv (Woodgate et al., 2012). The Pacific water influences the Arctic basin in a number of important ways. The cold winter water ventilates the interior halocline (e.g. Pickart et al., 2005) and provides nutrients that spur primary production (e.g. Codispoti et al., 2005). The summer water is a predominant source of heat and freshwater (e.g. Shimada et al., 2001; Yamamoto-Kawai et al., 2008). Over the last decade the heat and freshwater flux through Bering Strait has increased (Woodgate et al., 2012) and the warm Pacific water, which typically resides just below the surface mixed layer in the Canada Basin, has significantly contributed to both sea-ice melt in summer and a decrease in sea-ice formation during winter (Shimada et al., 2006). As such, the warm Pacific water has attracted great attention in recent years.

After entering the Chukchi Sea, the Pacific water follows three topographically steered branches across the shelf before reaching the deep Arctic basin (Fig. 1). The eastern branch flows adjacent to the Alaskan coast before exiting the Chukchi Sea through Barrow Canyon (Weingartner et al., 1998, 2005; Pickart et al., 2005). The middle branch flows through Central Channel between Herald and Hanna Shoals (Weingartner et al., 2005), and the western branch progresses

* Corresponding author.
E-mail address: motoyo@jamstec.go.jp (M. Itoh).

http://dx.doi.org/10.1016/j.dsr.2015.04.004

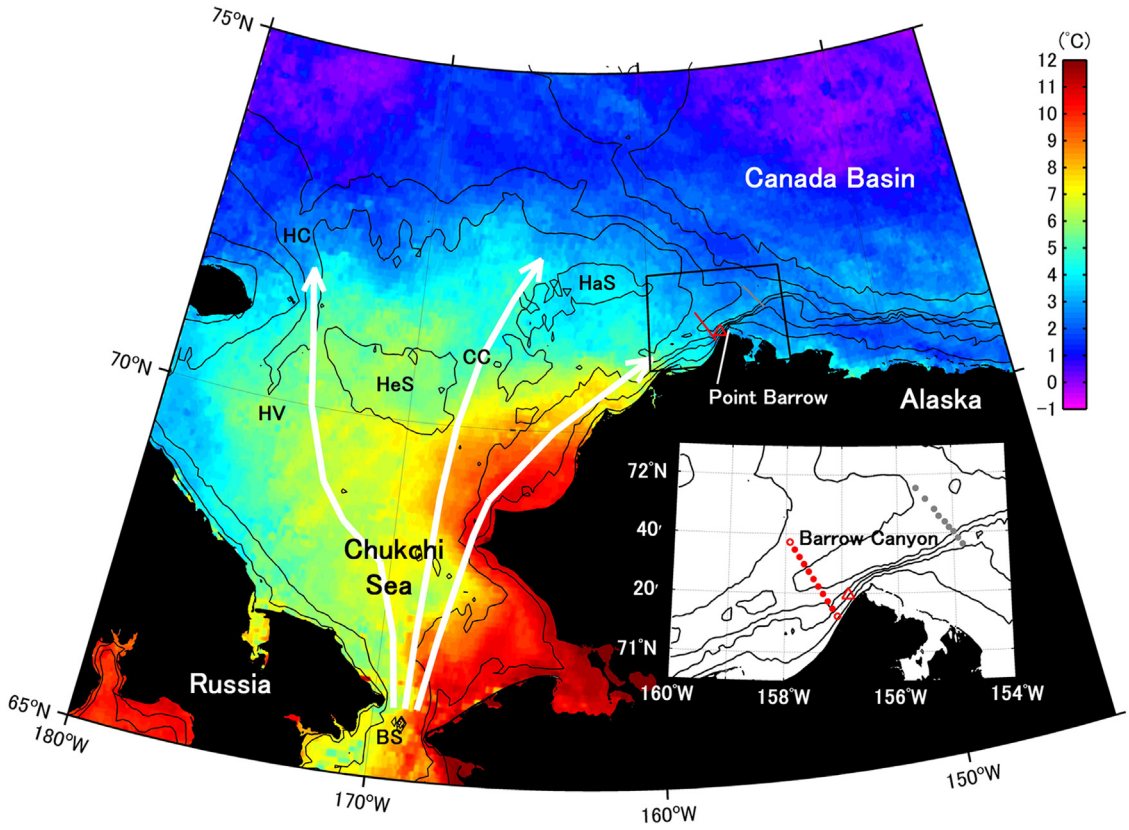

Fig. 1. Average sea surface temperature (color, °C) from the Moderate Resolution Imaging Spectroradiometer (MODIS) during 5 – 11 September 2010. The major topographic features of the Chukchi Sea from the International Bathymetric Chart of the Arctic Ocean (IBCAO, version 1.0) are overlaid. The black lines denote the 20, 40, 60, 80, 100, 500 and 2000 m isobaths. Bering Strait, Central Channel, Herald Canyon, Herald Valley, Herald Shoal, and Hanna Shoal are denoted by BS, CC, HC, HV, HeS, and HaS, respectively. The white arrows show schematic pathways of the Pacific water across the shelf. The black rectangular region indicates the region of the enlarged map around Barrow Canyon. Solid and open red circles indicate the stations of the DBO-5 repeat hydrographic transects conducted by the international research vessels listed in Table 1. Volume, freshwater and heat fluxes listed in Table 2 and heat and freshwater contents listed in Table 3 were integrated over the stations indicated by solid red circles. The location of the mooring Stn. B1 used in the study is denoted by the red triangle. Gray circles mark the location of transport measurements at the mouth of Barrow Canyon used in Fig. 6a.

through Herald Canyon on the western shelf (Woodgate et al., 2005; Pickart et al., 2010). In summer and early fall, when the volume and heat fluxes through Bering Strait increase to their maximum values, much of the inflowing water flows along the eastern branch as the Alaskan Coastal Current (ACC) (Paquette and Bourke, 1974). Furthermore, part of the Central Channel branch is believed to be diverted to the northeastern part of the shelf (Weingartner et al., 2013). Itoh et al., (2013) argued that the transport through Barrow Canyon accounts for roughly 94% of the Bering Strait transport during the months of July – September, and Gong and Pickart (2015) came to a similar conclusion using velocity data across the shelf. Therefore, Barrow Canyon is an ideal location to monitor Pacific water during the summer, especially for evaluating the heat flux into the Arctic basin.

Barrow Canyon represents a deep (extending to 300 m) and wide (50 km) incision into the Chukchi shelf that runs nearly parallel to the coastline of northwest Alaska. During the summer season, a number of Pacific-origin waters from Bering Strait can be found in the canyon (see for example Munchow and Carmack, 1997; Gong and Pickart, 2015), which can be divided into summer and winter waters. The two summer waters are the warm and fresh Alaskan coastal water (ACW, e.g. Paquette and Bourke, 1974) and the generally cooler and saltier summer Bering Sea water (BSW, e.g. Steele et al., 2004)[1]. Two classes of winter water have been distinguished in the literature based on a temperature criterion (e.g. Gong and Pickart, 2015), but in this study we make no such distinction and consider a single cold, relatively saline water mass referred to as Pacific winter water (PWW, e.g. Weingartner et al., 1998; 2005). The ACW flows predominantly along the coastal pathway, while the BSW is advected both near the coast and in the central pathway (Gong and Pickart, 2015). These two water masses are generally found in the upper part of the water column. During the summer months PWW drains into the canyon from the central shelf, constituting the last vestiges of the previous winter's convective product (E. Shroyer, pers. comm., 2014). This dense water is typically found at depth in the canyon below the summer waters, even as late as August (Pickart et al., 2005; Itoh et al., 2012).

Mooring observations in Barrow Canyon have revealed persistent northward flow that is strong in summer and weak in winter (Aagaard and Roach, 1990; Weingartner et al., 1998; 2005). The mean flow through Barrow Canyon is primarily forced by the sea-surface pressure gradient between the Pacific and Arctic Oceans, with variations mainly caused by changes in local wind (Weingartner et al., 2005; Woodgate et al., 2005; Itoh et al., 2013). During summer and fall, ship-based synoptic observations of the hydrography and circulation in Barrow Canyon were examined by Munchow and Carmack (1997), Weingartner et al. (2005), Pickart et al. (2005), Okkonen et al. (2009), Shroyer and Plueddemmann (2012), and Itoh et al., (2013). Furthermore, the seasonal and interannual variation of volume, freshwater, and heat flux through Barrow Canyon was examined using mooring observations at the mouth of the canyon from 2000 to 2008 (Itoh et al., 2013). The year-to-year variation in heat flux (relative to the

[1] Summer Bering Sea water has also been called western Chukchi summer water (Shimada et al., 2001) and Chukchi summer water (von Appen and Pickart, 2012).

freezing point) was substantial, ranging from 0.93 TW to 3.02 TW for 2006 and 2007, respectively (the 2007 value was a record maximum). The recent increase in summer heat flux through Bering Strait (Woodgate et al., 2012), combined with the fact that surface water is heated locally in the Chukchi Sea due to the enhanced sea ice retreat (Perovich et al., 2007; Perovich et al., 2008), implies that the heat flux through Barrow Canyon should be increasing. This in turn could significantly impact the basin, especially in light of the increased easterly winds in this region during summer (Pickart et al., 2013). Brugler et al. (2014) show that the export of Pacific water out of Barrow Canyon is more apt to flow directly northward into the Canada Basin under such wind conditions, rather than progressing eastward in the shelf-edge current of the Beaufort Sea (or on the Beaufort shelf). Watanabe (2011) argues that northward Ekman transport also redirects the warm Pacific water northward under enhanced easterly winds. However, the heat flux time series measurements presented by Itoh et al. (2013) only extend to 2008. Furthermore, their mooring observations were suspended from September 2008 to September 2010. Therefore, the summer heat flux thorough the Barrow Canyon in recent years is still unknown.

In this paper we investigate the flow of Pacific water through Barrow Canyon during summer 2010 using a series of 6 repeat, high-resolution shipboard transects occupied across the canyon from mid-July to late-September. The sections were done as part of the international project entitled the Distributed Biological Observatory (DBO, http://www.arctic.noaa.gov/dbo/). DBO designated five locations in the Pacific Arctic domain, spanning the latitudinal range from the northern Bering Sea to the northern Chukchi Sea, as important locations for ecosystem monitoring. The present work focuses on the northern-most DBO line located in Barrow Canyon. We also obtained time series data from a mooring deployed in the pathway of the Pacific summer water. Using the repeat hydrographic and velocity transects, together with mooring data, we investigate the intra-seasonal variation of the water masses and flow field in Barrow Canyon and present quantitative estimates of the volume, freshwater and heat fluxes through the canyon.

2. Data and methods

The concept behind the DBO is for ships of opportunity to carry out measurements at a set of sites ranging from the area near St. Lawrence Island in the northern Bering Sea to Barrow Canyon in the northeast Chukchi Sea. Depending on the type of cruise and the time available, the measurements range from basic physical observations to chemical and biological sampling of both the sea floor and the water column. When possible, a transect is occupied consisting of set of closely spaced stations at specified locations. DBO began its pilot phase in 2010, and during that summer the Barrow Canyon section (DBO line 5) was occupied 6 times from mid-July to late-September 2010 (Table 1). The section is typically comprised of 9 stations at 5 km horizontal spacing spanning the canyon (Fig. 1), and on all cruises except survey II, conductivity-temperature-depth (CTD) casts were done at each of the stations (the remaining cruise occupied only four of the CTD stations). Additional near-shore and offshore stations were done in surveys IV and V, respectively.

Each of the cruises used a Sea-Bird Electronics CTD with a SBE03 temperature sensor and SBE04 conductivity sensor. Pre-cruise laboratory calibrations of these sensors were done in each case, ranging from 4 to 8 months before the measurements were collected. It is typical for cruises sampling in deep water to perform an in-situ calibration of the conductivity sensor as well. However, because all of the cruises took place in shallow water (where vertical property gradients are strong), the bottle data could not be used to do reliable in-situ salinity calibrations. To examine the general accuracy of the temperature and conductivity sensors used, we considered data from six Arctic cruises of *R/V Mirai* from 2004 to 2013. In particular, we compared records from a collection of SBE03 and SBE04 sensors with highly accurate temperature and salinity data from SBE35 temperature recorders and water samples analyzed by a Guildline Autosal salinometer. The maximum half-yearly drift of the 12 SBE03 and 9 SBE04 sensors considered was 0.002 °C and 0.01, respectively. We take this as an overall measure of the uncertainty of the sensors used in our analysis, which is far smaller than the signals of interest in Barrow Canyon. Velocities were measured using acoustic Doppler current profilers (ADCPs) either mounted to the ship's hull, attached to the CTD package, or towed. Accuracies were assessed during the processing for each cruise and were found to be 2 cm s^{-1} for surveys I and V, 4 cm s^{-1} for survey II, 5 cm s^{-1} for survey IV, and 1 cm s^{-1} for survey VI. These errors are small relative to the mean velocity in Barrow Canyon (13–50 cm s^{-1}).

Nutrients were measured on five of the six surveys (no nutrient data were collected on survey III). However, on survey IV no water samples were collected below 50 m, and on survey VI nutrients were not obtained at every station. Despite these limitations, the data coverage was sufficient to help identify the different water masses present in the canyon during the summer (see Section 3 below). Measurement techniques differed on the cruises. For survey I the water column samples were analyzed at sea for nitrate (NO_3^-) and nitrite (NO_2^-) concentrations with a Seal Analytical continuous-flow AutoAnalyzer 3 (AA3) using a modification of the procedure by Armstrong et al. (1967). On surveys II, IV, and V the water samples were frozen and brought back to shore for analysis. For survey II, the nutrient samples were analyzed following the methods described in Barwell-Clarke and Whitney (1996). For survey IV, the analyses were performed using a hybrid Technicon AutoAnalyzer IITM and Alpkem RFA300TM system following protocols modified from Gordon et al. (1995). For survey V, the analyses were carried out using an Alpkem Rapid Flow Analyzer 300 following the protocols of Mordy et al. (2010). On survey VI the water samples were analyzed at sea following the GO-SHIP Repeat Hydrography procedure (Hydes et al., 2010) using the Reference Materials of Nutrients in Seawater (Aoyama and Hydes, 2010; Sato et al., 2010).

We also use mooring data in the study. A mooring was maintained from August 2009 to August 2011, consisting of an ADCP (Teledyne

Table 1
List of the DBO-5 repeat hydrography surveys.

Section	Vessel	Country	Start–end date, time (month/day/year, UTC)	Sea Bird CTD System	RD instruments ADCP
I	USCGC Healy	USA	07/12/10, 1730–07/13/10, 1050	SBE 911 plus	Vessel mounted Ocean Survey or 150 kHz
II	CCGS Sir Wilfrid Laurier	Canada	07/19/10, 1300–07/21/10, 2020	SBE 911 plus	Towed Broad Band 150 kHz
III	R/V Xue Long	China	07/25/10, 0850–07/25/10, 1700	SBE 911 plus	–
IV	R/V Annika Marie	USA	08/24/10, 1440–08/25/10, 0030	SBE 19 plus	Towed Work Horse Sentinel 300 kHz
V	USCGC Healy	USA	09/07/10, 2200–09/08/10, 0530	SBE 911 plus	Vessel mounted Ocean Surveyor 150 kHz
VI	R/V Mirai	Japan	09/28/10, 0000–09/29/10, 0630	SBE 911 plus	CTD mounted Work Horse Sentinel 300 kHz

Sentinel WH-300), a conductivity – temperature recorder (SBE37), and a temperature – pressure recorder (SBE39), all situated at roughly 36 m below the sea surface. The mooring, referred to as Stn. B1, was close to the DBO-5 line at a water depth of 42 m (see Fig. 1). Based on the DBO-5 shipboard transects, this location is within the core of the warm Pacific water during the summer season (see Section 3 below). The time series data obtained by the mooring were useful for measuring intra-seasonal variations of water properties and velocity, although the mooring observations could not provide hydrographic information in the upper 30 m because of the possibility of damage from ice keels. This demonstrates the value of having repeat hydrographic sections across the canyon that span the entire water column from the surface to the bottom, especially during summer when gradients of temperature and salinity are particularly strong within the upper layer.

To examine the relationship between currents and winds, we used meteorological data from the weather station of the Atmospheric Radiation Measurement (ARM) Climate Research Facility, Pt. Barrow, Alaska, USA. As part of our study we calculate the correlation between time series of along-canyon current and along-coast wind speeds. The effective number of degrees of freedom, which is needed for examining the significance level of the correlation, were derived following Davis (1976) and found to be 3, 3, 3, 9 and 5 for the months of June through October, respectively. Finally, we use CTD data from the Canada Basin obtained by *R/V Mirai* and *CCGS Louis S St-Laurent* from September through October 2010. Detailed descriptions of these data sets are found in Itoh (2010) and Williams (2010).

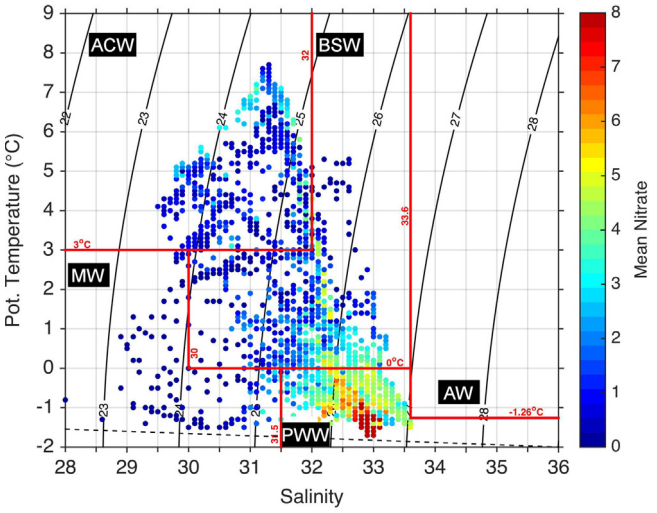

Fig. 2. Temperature/Salinity diagram using the water sample data from the DBO-5 surveys, where color represents nitrate concentration (μmol L^{-1}). The data were averaged within bins of 0.1 °C in temperature by 0.1 in salinity. The red lines denote the boundaries of the different water masses considered in the study, and the numbers are the corresponding temperature and salinity values of the boundaries. The water masses are: ACW = Alaskan coastal water; BSW = summer Bering Sea water; PWW = Pacific winter water; MW = sea-ice melt water; AW = Atlantic water. The AW boundaries are from Nikolopoulos et al. (2009) who used a year-long mooring data set to determine the Pacific/Atlantic interface (note: there was no AW measured in any of the 2010 DBO-5 surveys). The dashed line is the freezing line.

3. Synoptic hydrographic and flow fields during summer 2010

We begin by describing the water properties and current fields obtained from the 6 repeat hydrographic surveys of DBO-5 from mid-July to late-September, 2010. Satellite images from the Advanced Microwave Scanning Radiometer–EOS (AMSRE; not shown) indicate that the Barrow Canyon region was covered by sea ice in mid-July (surveys I and II) and that the ice edge was close to the canyon in late-July (survey III). The ice edge was more than 300 km north of the study area in late-August and September (surveys IV – VI).

The different water masses that were present in the canyon can be characterized by their temperature, salinity, and nutrient content. PWW tends to be elevated in nitrate because, as the dense water flows northward, it is in contact with the sediments which contain high levels of inorganic nutrients (e.g. Nishino et al., 2005; Mills et al., 2015). BSW is also relatively high in nitrate because one of its constituents, Anadyr water, becomes nutrient rich during the upwelling process in the Gulf of Anadyr (Springer et al., 1996; Wang et al., 2009). The Pacific water with the lowest nutrient content is ACW, although at times it can have modestly high levels of nitrate.

During the 2010 occupations of the DBO-5 section there were limited measurements of nutrients (none in survey III), but the coverage was enough to sample the different Pacific water masses. Using a Laplacian – Spline interpolator we made vertical sections of nitrate that objectively filled the data gaps, from which we constructed a composite temperature/salinity/nitrate plot (Fig. 2). Using this information, with guidance from historical definitions of water masses in the Chukchi Sea (e.g. Coachman et al., 1975), we defined boundaries of the different water types observed in the collection of sections. As seen in Fig. 2, the PWW contains the highest nitrate concentrations, followed by the BSW (even some of the ACW had slightly elevated concentrations). We stress that the boundaries in Fig. 2 are not precise and likely change over time, but, based on the vertical distributions of these water masses in the DBO-5 crossings, the definitions used here are reasonable. We note that there was no Atlantic water sampled during any of the surveys. There was, however, melt water (labeled MW in Fig. 2) found at the western end of some of the sections, confined to depths shallower than 30 m.

The occurrence of the different water masses through the summer season are documented in Fig. 3, which shows a temperature/salinity (T/S) histogram plot for each survey. This, together with the vertical sections of hydrographic variables (potential temperature, salinity, and potential density, Figs. 4 and 5) reveal quite marked changes in the water column as the season progresses. During the first part of the summer BSW was the dominant warm water mass in the canyon, but by survey IV (in late-August) ACW became more prevalent, reaching temperatures as high as 7.5 °C. By the time of the last survey (in late-September) the ACW was being cooled due to atmospheric forcing. Melt water was only present during the first three surveys, consistent with the satellite sea-ice concentration fields noted above which indicated that the ice edge was far north of the canyon during the last three surveys.

The two warm Pacific waters were located predominantly on the southeastern flank of Barrow Canyon, typically confined to within 10–20 km of the coast (Figs. 4 and 5). The ADCP velocity data reveal that the flow in this region was usually to the northeast (Fig. 6), although it varied from survey to survey. This was largely due to the wind, which is not surprising based on previous studies that have demonstrated a high sensitivity of the ACC to wind forcing (e.g. Okkonen et al., 2009; Gong and Pickart, 2015). The ACC was strongest ($\sim$0.9 m s^{-1}) during transect I when the winds were predominantly out of the west (Fig. 6a), while one week later, during survey II, the northeastward flow of the ACC had weakened considerably associated with a change in wind direction from westerly to easterly (Fig. 6b). However, wind forcing does not explain all of the variability in the transects. For example, the ACC was moderately weak during transect VI even though the winds were westerly at that time (as they were during transect I when the ACC was strong). There was also evidence of lateral displacements of the ACC; during surveys IV and V the axis of the current was displaced slightly offshore (Fig. 6d and e).

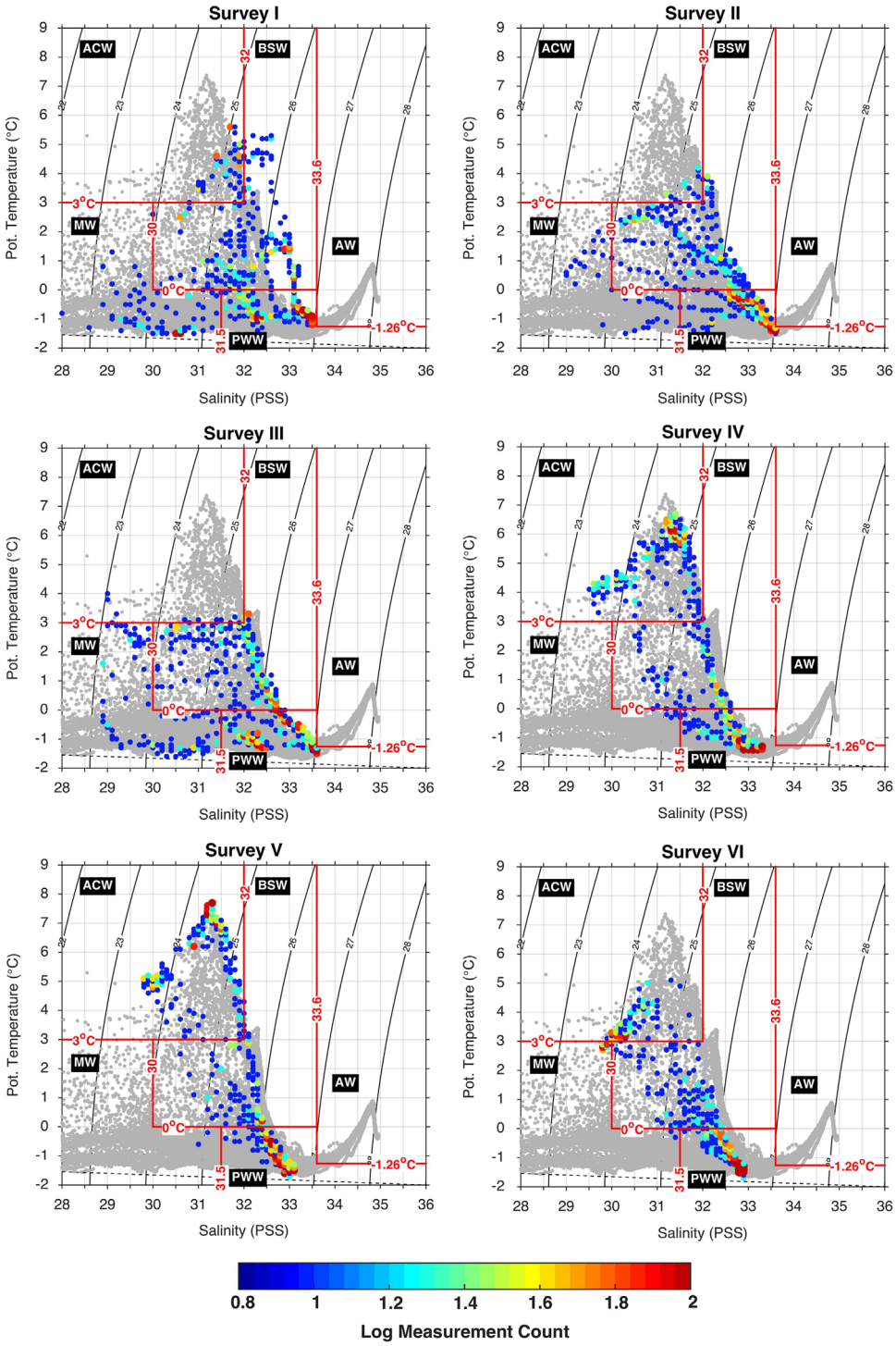

Fig. 3. T/S histogram plots for each of the DBO-5 surveys, where the number of occurrences in each bin is colored (in log counts). The bin size is 0.1 °C in temperature and 0.1 in salinity. The red lines are the water mass boundaries (see Fig. 2). Grey dots are T/S values observed in the Canada Basin (70–80°N, 130–160°W) with bottom depths greater than 1000 m in September and October 2010.

The winter water in Barrow Canyon also varied through the season. Close inspection of the T/S histogram plot (Fig. 3) reveals that there were two modes of PWW present in Barrow Canyon during 2010. One mode is characterized by salinities in the range of 32–33, and the other has a salinity near 33. These are referred to hereafter as low-salinity and high-salinity PWW. Both modes were observed in the early surveys (I – III), but by the later surveys only the fresher mode was present (particularly in surveys IV and V). The vertical sections reveal differences in the locations and velocity of the two PWWs. In particular, high-salinity PWW was present in the central part of the canyon, associated with relatively strong northeastward flow. In contrast, low-salinity PWW was prevalent on the northwestern side of the canyon, corresponding with generally weaker poleward flow.

These results suggest that the pathways of the high-salinity and low-salinity PWW approaching Barrow Canyon differed, resulting in the different salinities. In particular, the pathway along the Alaskan coast is the fastest of the Pacific water branches in the Chukchi Sea,

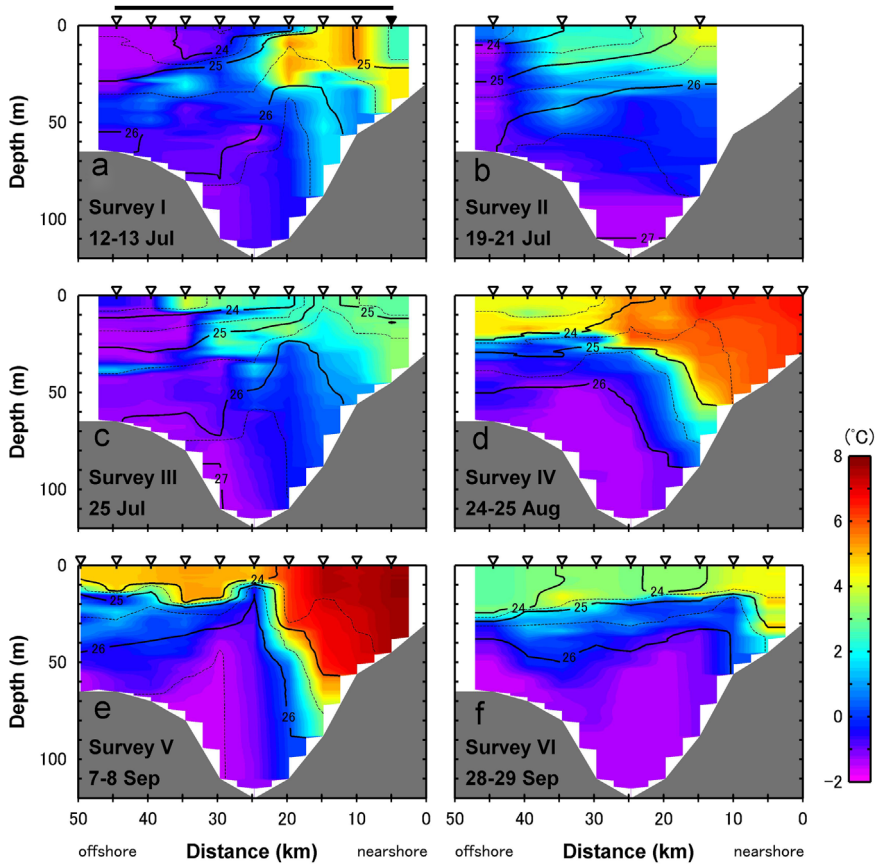

Fig. 4. Vertical sections of potential temperature (color, °C) and potential density (contours, kg m^{-3}) for the DBO-5 repeat hydrographic transects listed in Table 1. The viewer is looking north. Triangles at the top of each panel indicate CTD station locations. Stations below the black solid line in (a) were used for the integration of property fluxes and inventories on DBO-5 line in Tables 2 and 3. The location of mooring Stn. B1 is indicated by solid triangle in (a).

and would be subject to local salinization by the northeast Chukchi coastal polynya (Cavalieri and Martin, 1994; Iwamoto et al., 2014) in addition to smaller leads opening up along the coast. This implies that the high-salinity PWW entered Barrow Canyon through this pathway. In contrast, low-salinity PWW was most prevlant later in the season and was likely less influenced by salinization in the coastal polynya. This is consistent with an interior shelf pathway, possibly via the Central Channel then subsequently flowing cyclonically around Hanna Shoal before entering Barrow Canyon (Spall et al., 2008). We note that a very small amount of low-salinity PWW in surveys II and V was flowing southward on the westward edge of the canyon (0.02 Sv and 0.04 Sv, respectively). This water was possibly recirculated after leaving the canyon, or entered the canyon via the Chukchi shelfbreak jet (originating from Herald Canyon, Pickart et al., 2010). A long-term mooring in Barrow Canyon from 2000 to 2006 also revealed high-salinity PWW exiting the Chukchi Sea until August (Itoh et al., 2012), which is consistent with our results.

4. Volume and heat fluxes during summer 2010

In this section we examine the volume, freshwater, and heat fluxes through Barrow Canyon. The reference temperature used to calculate heat content and heat flux is the freezing temperature of seawater (dependent on salinity), as we are interested in the heat available for melting sea ice. We used $S=34.8$ as a reference salinity to calculate the freshwater content and freshwater flux, following Aagaard and Carmack (1989). Net property fluxes and contents were computed over the 9 stations spanning a 40 km distance across the canyon, indicated by the solid line in Fig. 4 and solid circles in the inset to Fig. 1. To simplify the results we considered two broad water classes: Pacific summer water (i.e. the BSW and ACW combined, which henceforth is referred to as PSW) and Pacific winter water (i.e. the combination of the low-salinity PWW and high-salinity PWW). Melt water was excluded from the calculations. We note that the ADCP does not measure currents within 5–20 m of the surface, and, for the depths of the DBO-5 section, the ADCP bottom blanking region varies from 5 to 17 m above the seafloor. Also, the CTD only measured temperature and salinity to within 2–10 m of the bottom. We filled in the missing hydrographic and velocity information using constant extrapolation. This was deemed reasonable even for the relatively large surface blanking region of the ADCP (~20 m), since the mooring data from Stn. B1 revealed a difference in along-canyon velocity between 7 m and 23 m of only ± 2 cm s^{-1} for July through September. We did not compute property fluxes and content for surveys II or III. In the former case, data were not obtained on the southeastern flank of the canyon where the PSW and strong currents exist. In the latter case, velocity data were not available for the section.

The calculated the fluxes from the DBO-5 repeat hydrographic/velocity sections are presented in Table 2[2]. The net volume transport through the canyon was poleward and varied between 0.96 and 1.70 Sv, consisting of 0.41–0.98 Sv of PSW and 0.28–0.65 Sv of PWW. The highest transport was observed in survey I, when the winds were strongly out of the west (Fig. 6a). The freshwater content showed small variations for all surveys. Thus,

[2] If we extrapolate the velocities and hydrographic variables to the coast (using constant extrapolation), the volume, freshwater, and heat fluxes are only increased by 1.2–1.7%, 1.5–2.5%, 2.3–4.6%, respectively.

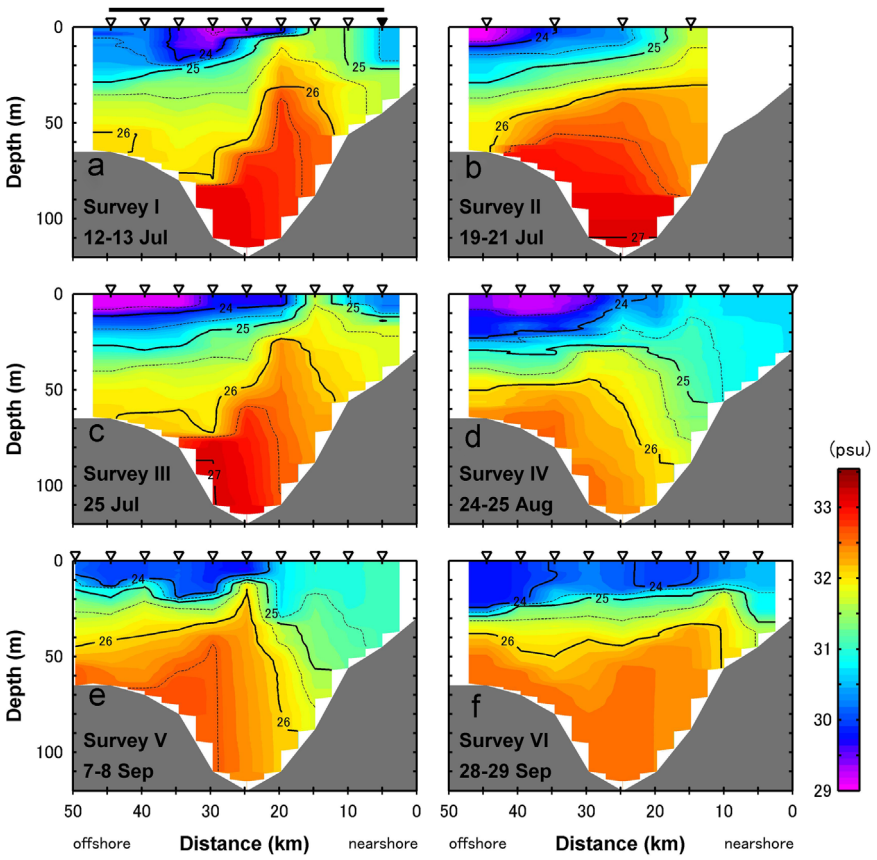

Fig. 5. Same as Fig. 4, except for salinity (color).

freshwater flux was mainly dictated by the volume flux, which is consistent with the mooring results of Itoh et al. (2013). Relatively large freshwater fluxes were observed in surveys I and IV, mainly due to the large volume transport through Barrow Canyon during those occupations. Heat content varied widely, ranging from 31.5 to 61.2 MJ between July and September. The PSW accounted for 70–92% of the total heat content. The maximum heat content was observed in early-September (survey V) when the temperature of ACW was the highest, almost twice as large as the values recorded in July (surveys I, III) and late-September (survey VI). The heat flux also varied strongly, ranging from 8.56 TW (survey VI in late-September) to 24.56 TW (survey V in early-September).

The variability of the flow in Barrow Canyon is largely dictated by along-coast winds (Weingartner et al., 2005; Woodgate et al., 2005; Itoh et al., 2013). As such, we examined the relationship between the winds at Pt. Barrow and the transport through the canyon using the DBO-5 repeat sections. We found that the maximum coherence occurred between along-canyon transport and nearly along-coast winds (75°T). In particular, easterly winds diminish the down-canyon transport and westerly winds enhance it. Four transport measurements from the mouth of Barrow Canyon (shown by gray dots in Fig. 1) were included in this analysis, in addition to the repeat DBO-5 surveys shown in Table 2. These additional surveys were conducted in September 2002, September 2010, September 2010, and July 2011 (see Itoh et al., 2013). It is reasonable to assume that the along-canyon transport is conserved over this short distance, consistent with the results of Pickart et al. (2005) who found little difference in transport between the head and mouth of the canyon. We note that both Pacific and Atlantic waters are present at the mouth of the canyon because the canyon depths (~300 m) are deeper than those of the DBO-5 section. Therefore, we used only the transport of Pacific water.

We compare Pacific water transport at the mouth of Barrow Canyon and along-coast winds at Pt. Barrow with a 12 h time-lag in Fig. 7a, since this resulted in maximum correlation. We note that the highest correlation occurs for 6.0–18.0 h time-lags. Disturbances in the current initiated by the wind should propagate northeastward along the Alaskan coast as coastally-trapped waves. For the above lags, this corresponds to wave speeds of 1.1–3.2 m s^{-1} for the distance from the Pt. Barrow weather station site to the mouth of the canyon. These speeds are similar to the topographic Rossby wave speed of 2.0 m s^{-1} found by Signorini et al. (1997) for approximated shelf-slope topography and forcing in Barrow Canyon. It is also consistent with the wave speeds of the three highest coastally-trapped modes found by Nakayama et al. (2012) for realistic shelf-slope topography (0.9–4.74 m s^{-1}).

A comparison of the volume transport and along-coast wind speed is shown in Fig. 7a. The data are significantly correlated ($r=0.936$) at a confidence level of 99%, demonstrating the importance of wind forcing in the canyon. This is consistent with the results of previous studies (Weingartner et al., 2005; Woodgate et al., 2005; Itoh et al., 2013). Fig. 7a also shows the linear regression line from a least squares fit between the volume transport and along-coast wind speed. The Barrow Canyon volume transport (V) was approximated by a linear function of the along-coast wind speed (W) as follows:

$$V = 0.25W + 1.06 \quad (1)$$

The intercept of the linear regression line in Eq. (1) represents the transport without wind forcing, which is 1.06 Sv. This is similar to the no-wind value determined by Itoh et al. (2013) and by Gong and Pickart (2015).

Using the wind-transport regression we constructed a time series of volume transport at the DBO-5 line for the time period of June to October 2010 based on Pt. Barrow weather station data in Fig. 8b. To validate this result, we compared it with the time series of along-canyon current from the mooring located near the

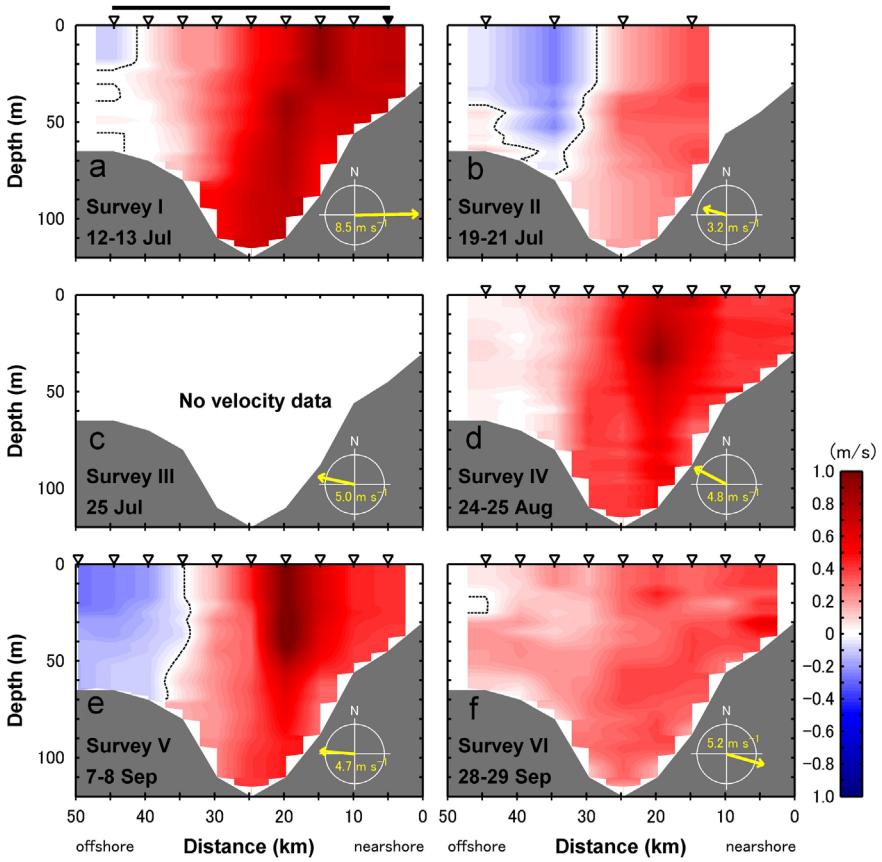

Fig. 6. Same as Fig. 4, except for velocity (color, m s^{-1}) measured by the different ADCPs (note that there was no velocity data for survey III). Northeastward down-canyon flow is positive. The dashed line is 0 m s^{-1} isotach. Included are the two-day averaged surface wind vectors at Pt. Barrow, centered at the time of occupation of each section. The compass circles indicate wind velocities of 4 m s^{-1}. Averaged wind velocity values for each cruise are indicated in yellow.

Table 2
Volume transport (Sv), freshwater flux (mSv), and heat flux (TW) across the DBO-5 line through the Barrow Canyon. Contributions of Pacific summer water (PSW) and Pacific winter water (PWW) are also listed. Definitions of PSW and PWW are shown in Fig. 2. Volume, freshwater and heat fluxes were integrated for 40 km width between stations indicated by solid red circles in Fig. 1 and solid black line in Fig. 2a. The uncertainty is due velocity error of 2 cm s^{-1} for surveys I and V, 5 cm s^{-1} for survey IV, and 1 cm s^{-1} for survey VI.

Survey	Volume transport (Sv)			Freshwater flux (mSv)			Heat flux (TW)		
	Total	PSW	PWW	Total	PSW	PWW	Total	PSW	PWW
I	1.70 ± 0.07	0.98 ± 0.03	0.65 ± 0.03	120.4 ± 5.9	76.3 ± 2.6	33.8 ± 1.9	21.21 ± 0.72	17.75 ± 0.54	3.09 ± 0.14
IV	1.31 ± 0.19	0.86 ± 0.11	0.44 ± 0.08	119.9 ± 17.4	89.6 ± 11.7	29.1 ± 5.0	22.62 ± 2.77	21.28 ± 2.51	1.28 ± 0.22
V	1.10 ± 0.08	0.83 ± 0.04	0.28 ± 0.03	93.7 ± 6.2	77.9 ± 4.3	16.4 ± 1.8	24.56 ± 1.22	23.91 ± 1.12	0.69 ± 0.10
VI	0.96 ± 0.04	0.41 ± 0.02	0.54 ± 0.02	77.7 ± 3.1	43.4 ± 1.7	33.2 ± 1.3	8.56 ± 0.34	6.87 ± 0.25	1.59 ± 0.06

Table 3
Freshwater content ($\times 10^5$ m^2) and heat content (MJ) across the DBO-5 line through the Barrow Canyon. Contributions of Pacific summer water (PSW) and Pacific winter water (PWW) are also listed. Temperature/Salinity diagram in Fig. 2 show definitions of PSW and PWW. Heat and freshwater contents were integrated stations indicated by solid red circles in Fig. 1 and solid black line in Fig. 4a.

Survey	Freshwater content ($\times 10^5$ m^2)			Heat content (MJ)		
	Total	PSW	PWW	Total	PSW	PWW
I	3.0	1.3	0.9	35.8	27.2	7.1
III	3.0	1.3	1.0	31.5	21.9	6.6
IV	3.5	2.3	1.0	55.4	50.3	4.4
V	3.1	2.2	0.9	61.2	56.1	4.8
VI	3.1	1.7	1.3	33.5	25.3	6.1

core of the PSW (see Fig. 1 for the location of the mooring). The significant correlation (r=0.743) between the wind-derived transport and the measured current is evident from June to October (compare Fig. 8b and c). We note that the correspondence lessens in late-September and October; this can be explained by changes in the current system and the water masses. In particular, the warm PSW disappears and colder water occupies the canyon this late in the season (Fig. 4f; see also Itoh et al. (2013)).

The average volume transport estimated using the wind data from July–September is 0.98 Sv, which is nearly equal to the unforced value from Fig. 7a. This is because, averaged over the summer season, the along-coast winds were relatively weak. Using long-term mooring records and wind data, Itoh et al. (2013) computed an interannual time series of transport in Barrow Canyon. Their value for July–September 2010 was 0.90, consistent with the value obtained here. For the DBO-5 data, the freshwater fluxes are highly correlated with volume fluxes (r=0.87, p=0.005), and were typically about 8.4% of the volume flux (not shown). The average freshwater flux estimated from the wind data for July–September is 82 mSv.

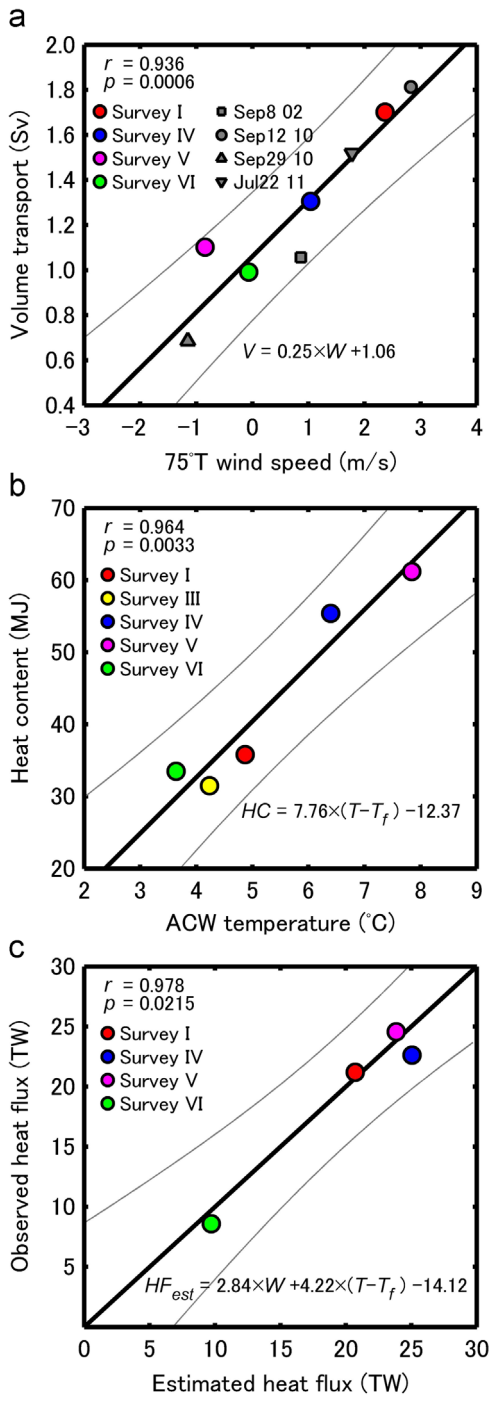

Fig. 7. Scatter plots showing the relationships between different variables in Barrow Canyon. The correlation coefficient (r) and p-value are indicated in the upper left corner of each panel. Statistical confidence of a nonzero correlation is given by $(1-p)$. The straight lines are least-squares regression lines. The thin curves show the 90% confidence bounds for estimated values from the regression analysis (cf. von Storch and Zwiers, 1999). See text for the equations of the lines in each panel. (a) Volume transport (Sv) through Barrow Canyon versus along-coast (75°T) wind speed (m/s) measured at the Pt. Barrow meteorological station. Gray symbols are volume transport observed at the mouth of Barrow Canyon. (b) PSW temperature (°C) at the mooring site versus heat content (MJ) at DBO-5 line. (c) Estimated heat flux (TW) from the multiple regression analysis versus the observed heat flux (TW) at DBO-5 line.

As mentioned above, PSW is the dominant source of heat in Barrow Canyon. We examined the relationship between the temperature measured by the mooring at the core of the PSW and the calculated heat content in Barrow Canyon at the DBO-5 line. A comparison of the heat content to the PSW temperature (relative to the freezing point, T_f) is shown in Fig. 7b. This demonstrates that the PSW temperature and the heat content are significantly correlated at the 99% level, and that the mooring time series of PSW temperature (Fig. 8d) can act as a proxy for the heat content in the canyon during the summer season. Fig. 7b also shows the linear regression line from a least squares fit between PSW temperature relative to the freezing temperature (T–T_f) and heat content (HC) as follows:

$$HC = 7.76(T - T_f) - 12.37 \quad (2)$$

We then used this proxy, along with the volume transport estimated from the along-coast wind (Fig. 8b), to obtain a measure of the heat flux in Barrow Canyon independent of the value calculated from the DBO measurements. In particular, we applied a multiple regression analysis of PSW temperature (T–T_f) and along-canyon wind (W) to estimate the heat flux in the canyon as follows:

$$HF_{est} = 2.84W + 4.22(T - T_f) - 14.12 \quad (3)$$

Fig. 7c shows the scatter plot of observed heat flux at DBO-5 line and estimated heat flux from Eq. (3), which demonstrates a favorable comparison. Unfortunately, only four of the DBO-5 repeat surveys could be used to test this relationship and more data are needed to fully verify it. Nonetheless, it suggests that variations in heat flux through Barrow Canyon can be explained by variations in PSW temperature and along-coast wind, and that our mooring-derived heat fluxes for July – September are realistic.

The estimated heat flux time series during July–September derived from the mooring data and the Pt. Barrow wind data is shown in Fig. 8e. The heat flux through Barrow Canyon was largest in September because of the presence of a relatively steady poleward volume transport (due to weak wind forcing) and the warmest PSW in the first half of September. The average heat flux during July–September was 13.4 TW, which corresponds to 1.1×10^{20} J of heat. This could melt 315,000 km^2 (560 km × 560 km) of 1-meter thick ice. We note that the temperature was mostly below 0 °C until the end of June and after the beginning of October (Fig. 8d), so the heat flux is very small for these periods. This suggests that most of the heat flux through the canyon occurs during the summer months, which is consistent with other studies. From the mooring results of Itoh et al. (2013), the difference between annual total heat flux and that from July to September ranges from −0.19–0.24 TW for 2001 – 2007, which is an order of magnitude smaller than annual total heat flux (1.97 TW). Also, farther to the east in the Beaufort shelfbreak jet, Brugler et al. (2014) found that nearly all of the heat flux occurred in the months of July-September. Thus, it is safe to assume that the integrated heat flux from July–September calculated here is comparable to the annual total heat flux through Barrow Canyon.

The average annual heat flux in 2010 was estimated to be 3.34 TW, which is as large as the 2007 record maximum for the time period 2001–2007 (Itoh et al., 2013), and 1.7 times larger than the average value during that period. One sees in Fig. 8e that the heat flux from late-August to mid-September was typically 20–40 TW. Notably, this is 3–5 times larger than that measured in 1993 (Munchow and Carmack, 1997), mainly due to an increase in temperature of the Pacific summer waters. Over the past few decades, Arctic sea ice cover has decreased dramatically (Stroeve et al., 2012). The sea ice extent in summer 2010 was the third lowest, next to 2007 and 2008, for the 30-year period 1979–2010. Local heating of surface water in the Chukchi Sea due to less sea ice during summer, together with the recent increased summer-time heat flux through the Bering Strait (Woodgate et al., 2012), likely both contributed to the warming of the PSW.

The increased heat flux through Barrow Canyon observed in 2007 and 2010 has likely contributed to the recent enhanced sea-ice melt in the Arctic basin. A significant portion of the Pacific

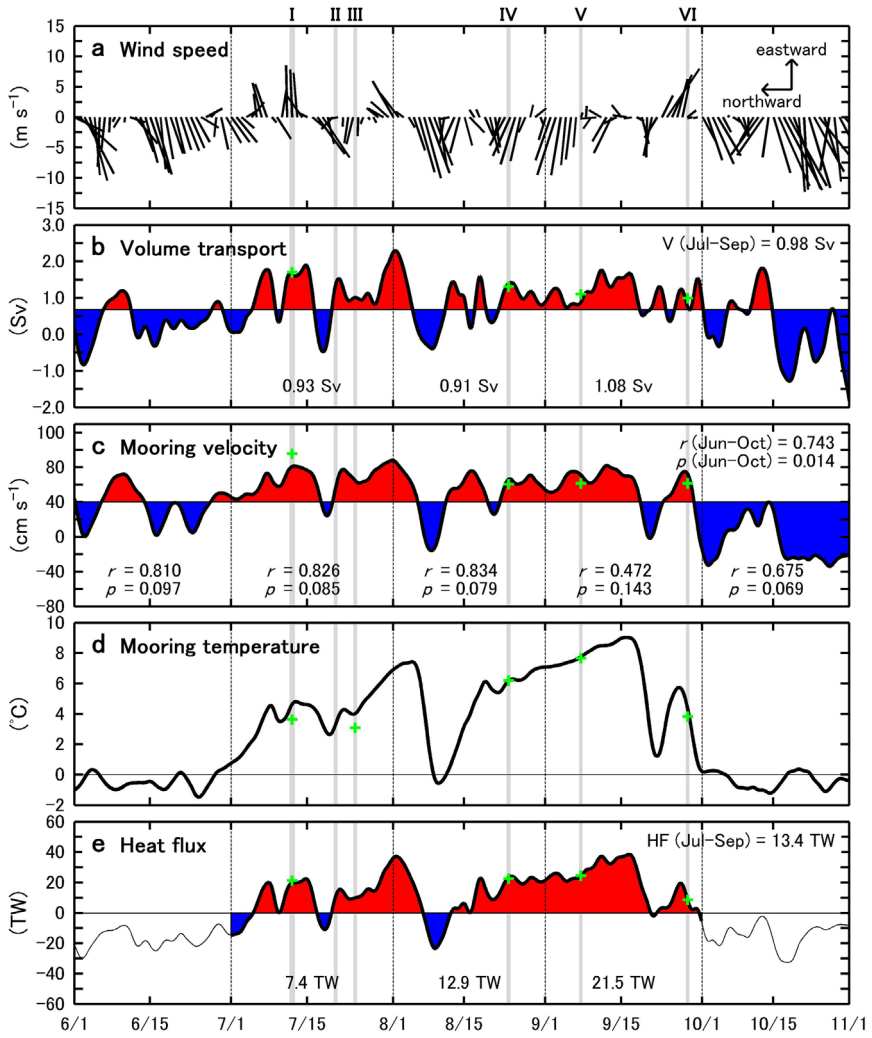

Fig. 8. Timeseries of various quantities in Barrow Canyon from June – October, 2010. The dates of the 6 DBO-5 occupations are indicated by the gray bars. (a) Wind speed ($m\,s^{-1}$) measured at the Pt. Barrow meteorological station. (b) Volume transport (Sv) across DBO-5 line estimated from the wind (northeastward down-canyon flow is positive). The green crosses indicate the measured values at the DBO-5 line. Higher (lower) than average values are indicated by the red (blue) shading. The monthly averaged values are indicated along the bottom of the panel, and the full summer average (July – September) is listed in the upper right of the panel. The standard error (cf. Emery and Thompson, 1997) of the estimated volume transport is ± 0.16 Sv. (c) Measured along-canyon velocity ($cm\,s^{-1}$). The correlation coefficients between the volume transport and along-canyon velocity (r) and p-value for each month are indicated along the bottom of the panel. The statistical confidence of a nonzero correlation is given by $(1-p)$. The correlation coefficient and p-value for the period June-October are indicated in the upper right of the panel. (d) PSW temperature (°C) from the mooring data. (e) Derived time series of heat flux (TW) across DBO-5 line (see text for details). The standard error of the estimated heat flux is ± 1.8 TW.

water that flows through Barrow Canyon is eventually transported into the Canada Basin by shelf-break eddies (Pickart 2004; Watanabe and Hasumi 2009), wind-driven Ekman flow (Pickart et al., 2013), or advection directly out of the canyon (Brugler et al., 2014).[3] While it is presently unknown which of these mechanisms is dominant, it is worth noting that in summer 2010 an anomalously warm and large anticyclonic ACW eddy containing 3.8×10^{18} J of heat was found in the southern Canada Basin (Nishino et al., 2011; Kawaguchi et al., 2012), corresponding to 3.5% of the total annual heat transport of PSW through the canyon.

5. Summary

Over the past few decades, sea ice retreat during summer has been enhanced in the Pacific sector of the Arctic basin, likely due in part to increased summertime heat flux of Pacific-origin water from the Bering Strait. Using data from 6 high-resolution shipboard sections across Barrow Canyon taken over the course of summer 2010, together with mooring data, we investigated the water masses and property fluxes through the canyon, which is a major conduit for Pacific water to spread into the interior Arctic basin. The different Pacific water masses feeding the canyon – Alaskan coastal water (ACW), summer Bering Sea water (BSW), and Pacific winter water (PWW) – all displayed significant intra-seasonal variability. The Alaskan Coastal Current (ACC) advected summer waters northward along the eastern flank of the canyon from mid-July to late-September. During the first three surveys the ACC contained mostly BSW, while in the latter three surveys it was comprised predominantly of ACW. PWW was typically found in the central and western parts of the canyon. The salinity of this

[3] A portion of the PSW flowing through Barrow Canyon may at times be advected onto the Beaufort shelf (Munchow and Carmack, 1997). However, this is far less than the amount transported by the Beaufort shelfbreak jet (Nikolopoulos et al., 2009).

water mass changed over the course of the season, with mostly higher salinity water flowing swiftly through the canyon in early summer, and lower salinity water flowing more slowly as the summer progressed. The high-salinity PWW would have been strongly influenced by salinization along the Alaskan coast, including the northeast Chukchi polynya, whereas low-salinity PWW would be less influenced by salinization via a pathway from Bering Strait to Barrow Canyon through the central Chukchi shelf.

Based on the repeat hydrographic/velocity sections, the net volume transport through the canyon was poleward, varying between 0.96 and 1.70 Sv. It consisted of 0.41–0.98 Sv of warm Pacific summer water (BSW and ACW) and 0.28–0.65 Sv of cold PWW. The heat flux varied widely, ranging from 8.56 to 24.56 TW, mainly due to the change in heat content of the summer water. The Barrow Canyon transport was linked to the local along-coast winds such that, under westerly winds, the volume flux through the canyon increased. The average volume transport estimated from the wind data for July–September was 0.98 Sv, which was nearly equal to the unforced transport estimated from the repeat shipboard sections. The amount of heat fluxed northward from July to September was 1.1×10^{20} J, which had the potential to melt 315,000 km^2 (560 km × 560 km) of 1-m thick ice. The annual average heat flux in 2010 was estimated to be 3.34 TW, which is as large as the record maximum observed previously in 2007 (Itoh et al., 2013). As such, this could have contributed significantly to the recent enhanced sea ice melt in the Pacific sector of the Arctic basin during summer and/or delayed ice formation during the fall and early winter.

Acknowledgements

We are greatly indebted to the officers and crew of the *USCGC Healy*, *CCGS Sir Wilfrid Laurier*, *R/V Xue Long*, *R/V Annika Marie* and *R/V Mirai*, and the scientists and technicians who collected the data. We sincerely thank Jackie Grebmeier, the lead investigator of the DBO program. Thanks are extended to Hajo Eicken, Andy Mahoney, the Barrow Arctic Consortium, UMIAQ, and the North Slope Borough Department of Wildlife Management for the mooring observations. Comments by Stephen Okkonen and two anonymous reviewers were very helpful for improving the manuscript. MI and TK thank Willam J. Williams and Andrey Proshutinsky who were the lead investigators of the *CCGS Louis S St-Laurent* cruise. CA thanks Robert G. Campbell and Stephen Okkonen, co-principal investigators of the project associated with the *R/V Annika Marie* cruise. MI acknowledges Amane Fujiwara for the MODIS SST processing. MI, RP, and CA are indebted to Frank Bahr for processing the shipboard ADCP data. MI and SN acknowledge Michio Aoyama for processing the nutrient data associated with the *R/V Mirai* cruise. MI, TK, YF, KO and DS were supported by Green Network of Excellence Program (GRENE Program), Arctic Climate Change Research Project 'Rapid Change of the Arctic Climate System and its Global Influences' by Ministry of Education, Culture, Sports, Science and Technology Japan. RP was supported by grant ARC-1203906 from the US National Science Foundation. CA was supported by grant ARC-1023331 from the US National Science Foundation and by the Cooperative Institute for the North Atlantic Region (NOAA Cooperative Agreement NA09OAR4320129) with funds provided by the US National Oceanographic and Atmospheric Administration through an Interagency Agreement between the US Bureau of Ocean and Energy Management and the National Marine Mammal Laboratory. SV was supported by the Department of Fisheries and Oceans Canada. MI and TK were supported by the Japan Agency for Marine-Earth Science and Technology. MI, TK, YF and KO were supported by Grant no. 2014-23 from Joint Research Program of the Institute of Low Temperature Science, Hokkaido University. YF and KO were supported by grants-in-aid 20221001 for scientific research from the Ministry of Education, Culture, Sports, Science and Technology of Japan. JTM was supported by grant PLR-1041102 from the US National Science Foundation.

References

Aagaard, K., Carmack, E.C., 1989. The role of sea ice and other fresh water in the Arctic circulation. J. Geophys. Res. 94, 14,485–14,498.

Aagaard, K., Roach, A., 1990. Arctic ocean-shelf exchange: measurements in Barrow Canyon. J. Geophys. Res. 95, 18,163–18,175.

Aoyama, M., Hydes, D.J., 2010. How do we improve the comparability of nutrient measurements?. In: Aoyama, M., et al. (Eds.), Comparability of Nutrients in the World's Ocean. Mother Tank, Tsukuba, Japan, pp. 1–10.

Armstrong, F., Stearns, C.R., Strickland, J., 1967. The measurement of upwelling and subsequent biological process by means of the Technicon Autoanalyzer® and associated equipment. Deep-Sea Res. 14, 381–389. http://dx.doi.org/10.1016/0011-7471(67)90082-4.

Barwell-Clarke, J., Whitney, F., 1996. Institute of ocean sciences nutrient methods and analysis. Can. Tech. Rep. Hydrogr. Ocean Sci. 182, 43, vi +.

Brugler, E., Pickart, R., Moore, G., Robert, S., Weingartner, T., Statscewich, H., 2014. Seasonal to interannual variability of the Pacific water boundary current in the Beaufort Sea. Prog. Oceanogr. , http://dx.doi.org/10.1016/j.pocean.2014.05.002.

Cavalieri, D.J., Martin, S., 1994. The contribution of Alaskan, Siberian, and Canadian coastal polynyas to the cold halocline layer of the Arctic Ocean. J. Geophys. Res. 634 (99), 18,343–18,362, C9.

Coachman, L.K., Aagaard, K., Tripp, R.B., 1975. Bering Strait. The Regional Physical Oceanography. University of Washington Press, Seattle and London p. 172.

Codispoti, L., Flagg, C., Kelly, V., Swift, J., 2005. Hydrographic conditions during the 2002 SBI process experiments. Deep-Sea Res. II 52 (24–26), 3199–3226.

Davis, R.E., 1976. Predictability of sea surface temperature and sea level pressure anomalies over the North Pacific Ocean. J. Phys. Oceanogr. 6, 249–266.

Emery, W., Thompson, R., 1997. Data analysis methods in physical oceanography. Elsevier Science B.V, 638.

Gong, D., Pickart, R.S., 2015. Summertime circulation in the eastern Chukchi Sea. Deep-Sea Res. II http://dx.doi.org/10.1016/j.dsr2.2015.02.006, in press.

Gordon, L.I., Jennings, J.C., Ross, A.A., Krest, J.M., 1995. A suggested protocol for continuous flow automated analysis of seawater nutrients (phosphate, nitrate, nitrite and silicic acid). In: The WOCE Hydrographic Program and the Joint Global Ocean Fluxes Study, WOCE Operations Manual, WOCE Report no. 68/91. Revision 1995.

Hydes, D.J., Aoyama, M., Aminot, A., Bakker, K, Becker, S., Coverly, S.,Daniel, A., Dickson, A., Grosso, O., Kerouel, R., Van Ooijen, J., Sato, K., Tanhua, T., Woodward, M., Zhang, J. Hydes, D.J., 2010. Determination of dissolved nutrients (N, P, Si) in seawater with high precision and inter-comparability using gas-segmented continuous flow analysers. In: Hood, E.M., Sabine, C.L., Sloyan, B.M. (Eds.), The GO-SHIP Repeat Hydrography Manual: A Collection of Expert Reports and Guidelines, ICPO Publication Series, vol. 134, IOCCP Rep. 14, United Nations Educational, Scientific and Cultural Organization. Intergovernmental Oceanographic Commission, IOC-UNESCO, Paris.

Itoh, M., 2010. R/V Mirai Cruise Report MR10-05, JAMSTEC, Yokosuka, Japan ⟨http://www.godac.jamstec.go.jp/cruisedata/mirai/e/index.html⟩.

Itoh, M., Shimada, K., Kamoshida, T., McLaughlin, F., Carmack, E.C., Nishino, S., 2012. Interannual variability of PWW inflow through Barrow Canyon from 2000 to 2006. J. Oceanogr. , http://dx.doi.org/10.1007/s10872-012-0120-1.

Itoh, M., Nishino, S., Kawaguchi, Y., Kikuchi, T., 2013. Barrow Canyon volume, heat, and freshwater fluxes revealed by long-term mooring observations between 2000 and 2008. J. Geophys. Res. Oceans 118, 4363–4379. http://dx.doi.org/10.1002/jgrc.20290.

Iwamoto, K., Ohshima, K.I., Tamura, T., 2014. Improved mapping of sea ice production in the Arctic Ocean using AMSR-E thin ice thickness algorithm. J. Geophys. Res. Oceans, 119. http://dx.doi.org/10.1002/2013JC009749.

Kawaguchi, Y., Itoh, M., Nishino, S., 2012. Detailed survey of a large baroclinic eddy with extremely high temperature in the Western Canada Basin. Deep-Sea Res. I 66, 90–102. http://dx.doi.org/10.1016/j.dsr.2012.04.006.

Mills, M.M, Brown, Z.W., Lowry, K.E., van Dijken, G.L., Becker, S., Pal, S., Benitez-Nelson, S., Strong, A.L., Swift, A.L., Pickart, R.S., Arrigo, K.R., 2015. Impacts of low phytoplankton NO_3^-:PO_4^{3} utilization ratios over the Chukchi Shelf, Arctic Ocean. Deep-Sea Res. II 10.1016/j.dsr2.2015.02.007, in press.

Mordy, C.W., Eisner, L.B., Proctor, P., Stabeno, P., Devol, A.H., Shull, D.H., Napp, J.M., Whitledge, T., 2010. Temporary uncoupling of the marine nitrogen cycle: accumulation of nitrite on the Bering Sea shelf. Mar. Chem. 121, 157–166. http://dx.doi.org/10.1016/j.marchem.2010.04.004.

Munchow, A., Carmack, E.C., 1997. Synoptic flow and density observation near an Arctic shelf break. J. Phys. Oceanogr. 27, 1402–1419.

Nakayama, Y., Ohshima, K.I., Fukamachi, Y., 2012. Enhanced of sea ice drift due to the dynamical interaction between sea ice and a coastal ocean. J. Phys. Oceanogr. 42, 179–192. http://dx.doi.org/10.1175/JPO-D-11-018.1.

Nikolopoulos, A., Pickart, R.S., Fratantoni, P.S., Shimada, K., Torres, D.J., Jones, E.P., 2009. The western Arctic boundary current at 152°W: Structure, variability, and transport. Deep-Sea Res. II 56, 1164–1181.

Nishino, S., Shimada, K., Itoh, M., 2005. Use of ammonium and other nitrogen tracers to investigate the spreading of shelf waters in the western Arctic halocline. J. Geophys. Res. Oceans 110 (C10), C10005. http://dx.doi.org/10.1029/2003JC002118.

Nishino, S., Itoh, M., Kawaguchi, Y., Kikuchi, T., 2011. Impact of an unusually large warm-core eddy on distributions of nutrients and phytoplankton in the southwestern Canada Basin during late summer/early fall 2010. Geophys. Res. Lett. 38, L16602. http://dx.doi.org/10.1029/2011GL047885.

Okkonen, S.R., Ashjian, C.J., Campbell, R.G., Maslowski, W., Clement-Kinney, J.L., Potter, R., 2009. Intrusion of warm Bering/Chukchi waters onto the shelf in the western Beaufort Sea. J. Geophys. Res. Oceans 114 (C00A11), http://dx.doi.org/10.1029/2008JC004870.

Paquette, R., Bourke, R., 1974. Observation on the coastal current of Arctic Alaska. J. Mar. Res. 32, 195–207.

Perovich, D., Light, B., Eicken, H., Jones, K., Runciman, K., Nghiem, S., 2007. Increasing solar heating of the Arctic Ocean and adjacent seas, 1979–2005: attribution and role in the ice-albedo feedback. Geophys. Res. Lett. 34, L19505. http://dx.doi.org/10.1029/2007GL031480.

Perovich, D., Ritcher-Menge, J., Jones, K., Light, B., 2008. Sunlight, water, and ice: extreme Arctic sea ice melt during the summer of 2007. Geophys. Res. Lett. 35 (L19595), http://dx.doi.org/10.1029/2008GL034007.

Pickart, R.S., 2004. Shelfbreak circulation in the Alaskan Beaufort Sea: mean structure and variability. J. Geophys. Res. 109, C04024. http://dx.doi.org/10.1029/2003JC001912.

Pickart, R.S., Weingartner, T., Pratt, L., Zimmermann, S., Torres, D., 2005. Flow of winter-transformed Pacific water direct measurement of transport and water properties through the Bering Strait. Deep-Sea Res. II 52, 3,175–3,198.

Pickart, R.S., Pratt, L.J., Torres, D.J., Whitledge, T.E., Proshutinsky, A.Y., Aagaard, K., Agnew, T.A., Moore, G.W.K., Dail, H.J., 2010. Evolution and dynamics of the flow through Herald Canyon in the Western Chukchi Sea. Deep-Sea Res. II 57, 5–26. http://dx.doi.org/10.1016/j.dsr2.2009.08.002.

Pickart, R.S., Spall, M.A., Mathis, J.T., 2013. Dynamics of upwelling in the Alaskan Beaufort Sea and associated shelf-basin fluxes. Deep-Sea Res. 76, 35–51.

Roach, A., Aagaard, K., Pease, C., Salo, S., Weingartner, T., Pavlov, V., Kulakov, M., 1996. Direct measurements of transport and water properties through the Bering Strait. J. Geophys. Res. 100, C9. http://dx.doi.org/10.1029/95JC01673.

Sato, K., Aoyama, M., Becker, S., 2010. Reference materials for nutrients in seawater as calibration standard solution to keep comparability for several cruises in the world ocean in 2000s. In: Aoyama, M., et al. (Eds.), Comparability of Nutrients in the World's Ocean. Mother Tank, Tsukuba, Japan, pp. 43–56.

Shimada, K., Carmack, E.C., Hatakeyama, K., Takizawa, T., 2001. Varieties of shallow temperature maximum waters in the western Canadian Basin of the Arctic Ocean. Geophys. Res. Lett. 28, 3441–3444.

Shimada, K., Kamoshida, T., Itoh, M., Nishino, S., Carmack, E.C., McLaughlin, F., Zimmermann, S., Proshutinsky, A., 2006. Pacific Ocean inflow: influence on catastrophic reduction of sea ice cover in the Arctic Ocean. Geophys. Res. Lett. 33, L08605. http://dx.doi.org/10.1029/2005GL025624.

Shroyer, E.K., Plueddemmann, A.J., 2012. Wind-driven modification of the Alaskan coastal current. J. Geophys. Res. 117, C03031. http://dx.doi.org/10.1029/2011JC007650.

Signorini, S., Munchow, A., Haidvogel, D., 1997. Flow dynamics of a wide Arctic canyon. J. Geophys. Res. 102, 18,661–18,680.

Spall, M.A., Pickart, R.S., Fratantoni, P.S., Plueddemann, A.J., 2008. Western Arctic Shelfbreak eddies: formation and transport. J. Phys. Oceanogr. 38, 1644–1668.

Springer, A.M, McRoy, C.P., Flint, M.V., 1996. The Bering Sea Green Belt: shelf-edge processes and ecosystem production. Fish. Oceanogr. 5, 205–223.

Steele, M., Morison, J., Ermold, W., Rigor, I., Orrmeyer, M., Shimada, K., 2004. Circulation of summer Pacific halocline water in the Arctic Ocean. J. Geophys. Res. 109, C02029. http://dx.doi.org/10.1029/2003JC002009.

Stroeve, J.C., Serreze, M.C., Holland, M.M., Kay, J.E., Maslanik, J., Barrett, A.P., 2012. The Arctic's rapidly shrinking sea ice cover: a research synthesis. Clim. Change 110, 1005–1027. http://dx.doi.org/10.1007/s10584-011-0101-1.

von Appen, W.J., Pickart, R.S., 2012. Two configurations of the western Arctic shelfbreak current in summer. J. Phys. Oceanogr. 42 (3), 329–351. http://dx.doi.org/10.1175/JPO-D-11-026.1.

von Storch, H., Zwiers, F.W., 1999. Statistical Analysis in Climate Research. Cambridge University Press, Cambridge, United Kingdom p. 484.

Wang, J., Hu, H., Mizobata, K., Saitoh, S., 2009. Seasonal variations of sea ice and ocean circulation in the Bering Sea: a model-data fusion study. J. Geophys. Res., 114. http://dx.doi.org/10.1029/2008JC004727.

Williams, J.W., 2010. Joint Ocean Ice Study (JOIS) 2010 Cruise Report ⟨http://www.whoi.edu/beaufortgyre/results⟩, Institute of Ocean Sciences, Sidney, B.C., Canada.

Weingartner, T., Cavalieri, D., Aagaard, K., Sasaki, Y., 1998. Circulation, dense water formation, and outflow on the northwest Chukchi shelf. J. Geophys. Res. 103, 7647–7661.

Weingartner, T., Aagaard, K., Woodgate, R., Danielson, S., Sasaki, Y., Cavalieri, D., 2005. Circulation on the north central Chukchi Sea shelf. Deep-Sea Res. II 52, 3150–3174.

Weingartner, T., Dobbins, E., Danielson, S., Winsor, P., Potter, R., Statscewich, H., 2013. Hydrographic variability over the northeastern Chukchi Sea shelf in summer-fall 2008–2010. Cont. Shelf Res. 67, 5–22. http://dx.doi.org/10.1016/j.csr.2013.03.012.

Woodgate, R., Aagaard, K., Weingartner, T., 2005. A year in the physical oceanography of the Chukchi Sea: moored measurement from autumn 1990–1991. Deep-Sea Res. II 52, 3116–3149.

Woodgate, R., Aagaard, K., Weingartner, T., 2006. Interannual changes in the Bering Strait fluxes in volume, heat and freshwater between 1991 and 2004. Geophys. Res. Lett. 33, L15609. http://dx.doi.org/10.1029/2006GL026931.

Woodgate, R., Weingartner, T., Linsay, R., 2012. Observed increases in Bering Strait oceanic fluxes from the Pacific to the Arctic from 2001 to 2011 and their impacts on the Arctic Ocean water column. Geophys. Res. Lett. 39, L24603. http://dx.doi.org/10.1029/2012GL054092.

Watanabe, E., Hasumi, H., 2009. Pacific water transport in the western Arctic Ocean simulated by an eddy-resolving coupled sea ice-ocean model. J. Phys. Oceanogr. 39, 2194–2211.

Watanabe, E., 2011. Beaufort shelf break eddies and shelf-basin exchange of Pacific summer water in the western Arctic Ocean detected by satellite and modeling analyses. J. Geophys. Res. 116, C08034. http://dx.doi.org/10.1029/2010JC006259.

Yamamoto-Kawai, M., McLaughlin, F., Carmack, E.C., Nishino, S., Shimada, K., 2008. Freshwater budget of the Canada Basin, Arctic Ocean, from salinity, $\delta^{18}O$, and nutrients. J. Geophys. Res. 113, C01007. http://dx.doi.org/10.1029/2006JC003858.